

Evidence of Enhanced Low Temperature Water-Gas Shift Rate with Sodium Promoted Pt/Zirconia-Based Catalyst Discovered by Combinatorial Methods

John M. Pigos¹, Christopher J. Brooks¹, Gary Jacobs², Burtron H. Davis²

¹*Honda Research Institute USA, Inc.
1381 Kinnear Rd.
Columbus, OH 43212 USA*

²*Center for Applied Energy Research
University of Kentucky
2540 Research Park Drive
Lexington, KY 40511 USA*

Introduction

For the successful commercialization of PEM fuel cells for portable power and transportation applications, there is a strong need to lower the amount of water-gas shift catalyst used within fuel processor for H₂ production/purification. While most recent studies have improved the current understanding of water-gas shift catalysis, especially regarding structural-property relationships and catalytic mechanism, a highly active and stable catalyst has remained elusive. With the advent of combinatorial approaches, however, this situation is improving.

In 2005, Brooks et al.¹ reported results of combinatorial screening of over 250,000 catalyst materials. One of the findings was that an important improvement in catalyst activity was realized when Pt/ZrO₂ was promoted with the alkali, Na. While ceria has received considerable attention as the partially reducible oxide component for low temperature shift catalysts,²⁻⁷ there are few reports in the literature for water-gas shift over ZrO₂-based catalysts. However, recently reported catalytic behavior for Pt/ZrO₂ suggests that defects (e.g. vacancies) in the surface of zirconium oxide could be generated with the presence of Pt.^{8,9} It is possible that these defects can form bridging OH groups, that once formed, have been proposed to react with CO to produce surface formates, as seen in ceria systems.^{2,6,7,10-12}

For ceria-based catalysts, while there is general agreement that surface reduction of ceria is important for the heterogeneous catalysis, there is still a debate as to how these defect sites function. On one hand, the partial reduction of ceria in H₂ has been proposed to lead to the formation of Type II bridging OH groups^{12,13}, and once formed they react with CO to produce surface formates. Also, they proposed that Pt⁰ facilitated the dissociation and spillover of hydrogen to the ceria surface, in order to reduce the ceria and form the Type II bridging OH groups directly. In the presence of H₂O, the formates decomposed much more rapidly, and in the forward direction, to yield H₂ and unidentate carbonate, which decomposed further to CO₂. Based on mechanistic studies, including kinetic isotope effect studies^{2,7} and isotope tracer studies¹⁴, it has been suggested that the rate limiting step of the surface formate mechanism involves cleaving the C-H bond of the formate for low temperature water gas shift.

Analogous bridging OH groups and surface formate species¹⁵⁻¹⁷ have been identified for thoria and zirconia-based catalysts. It has been noted that, doped with Pt metal, Pt/thoria¹⁸ and Pt/zirconia¹⁹ materials exhibit a much higher water-gas shift activity relative to the undoped oxides. This was attributed to a lower temperature for the bridging OH group activation, the formation of analogous formate species as observed for ceria, and a rapid forward decomposition of these formates in the presence of steam. Similar normal kinetic isotope effects were observed for these materials as seen previously for Pt/ceria, suggesting that the rate limiting step was likely the C-H bond scission of the formate intermediate.

In other reports, for ceria, it has also been proposed that the role of oxygen vacancies is not to activate H₂O by dissociative adsorption (as in the formate mechanism) but rather to directly replenish the O from the H₂O molecule. This results in reoxidizing the ceria and liberating H₂ in the process. The vacancy would be generated again by reaction of CO, chemisorbed on Pt, with O on the ceria surface at the interface, producing CO₂ in the process. This process is known as the ceria-mediated redox mechanism.³⁻⁵ In this work, the promoting effect of Na on Pt/ZrO₂ was examined in terms of the formate mechanistic perspective using DRIFTS. The aim of the current investigation was to determine whether or not the Na influenced the formate intermediate and to determine specifically if the turnover rate of the formate was enhanced during the water-gas shift.

Experimental

Catalysis Preparation Commercial high surface-area zirconium support Gobain NorPro, BET surface area of 117 m²/g, was impregnated with aqueous platinum and sodium salt containing solutions. The impregnated catalysts were dried in an oven at 110°C for 24 hours and then calcined at 300°C for 3 hours in a furnace. Sequential impregnations were carried out by drying and calcining after each metal addition.

BET surface area BET surface area measurements were carried out on Micromeritics TriStar 3000 gas adsorption analyzer. Approximately 0.35 g of sample was weighted out and loaded into a 3/8" inch sample tube. Nitrogen was used as the adsorption gas and sample analysis was performed at the boiling temperature of liquid nitrogen.

Temperature programmed reduction Temperature programmed reduction (TPR) was conducted on ZrO₂, Pt/ZrO₂, Na/ZrO₂, and PtNa/ZrO₂ catalysts using a Zeton-Altamira AMI-200 unit equipped with a thermal conductivity detector (TCD). The temperature range was 50 to 1100°C, and the ramp rate was 10 °C/min. Argon served as the reference gas, and 10 %H₂ in Ar was used as the treatment gas. The flow rate of the H₂ treatment gas was 30 cm³/min. The temperature of the catalyst was recorded from a thermocouple positioned inside the catalyst bed. Approximately 0.15-0.30 g of catalyst was utilized in each test.

Diffuse reflectance Fourier transform infrared spectroscopy The infrared spectrometer was a Nicolet Nexus 870, equipped with a DTGS-TEC detector. A chamber fitted with ZnSe windows capable of high temperature and high pressure served as the reactor for CO adsorption and water-gas shift experiments. The catalyst amount used was 40 mg.

Catalysts were activated with $\text{H}_2:\text{N}_2$ 100 $\text{cm}^3/\text{min}:$ 130 cm^3/min at 300°C, purged in N_2 130 cm^3/min , and cooled to a temperature of interest in N_2 to obtain background scans. Reference spectra were generated for formate species by adsorption of formic acid, while reference spectra for carbonate species were generated by adsorption of CO_2 . For CO adsorption measurements, $\text{CO}:\text{N}_2$ 3.75 $\text{cm}^3/\text{min}:$ 130 cm^3/min was flowed at 300°C and cooled to the temperature of interest. Following CO adsorption experiments, steady state water-gas shift measurements were carried out (300°C or 225°C) using $\text{CO}:\text{H}_2\text{O}:\text{N}_2$ 3.75 $\text{cm}^3/\text{min}:$ 62.5 $\text{cm}^3/\text{min}:$ 67.5 cm^3/min .

Results and Discussion

Temperature programmed reduction profiles are reported in Figure 1. Reduction of ZrO_2 support exhibited two distinct TPR peaks, both of which are most likely due to reduction in the surface shell, at ~ 440°C and 630°C, respectively. The reduction process involves both surface carbonate decomposition and uptake of hydrogen during formation of the Type II bridging OH groups. The addition of Pt caused a remarkable shift in the surface reduction process to lower temperature. A major asymmetric peak is observed at 175°C, with a pronounced shoulder at 140°C. With such systems as metal/ CeO_2 catalysts, it has been observed that reduction of Pt oxide occurs first, at a slightly lower temperature than that of the CeO_2 surface shell reduction⁷. Therefore, the lower temperature shoulder is most likely ascribed to reduction of Pt oxide to Pt^0 , while the more intense peak is due to reduction in the surface shell of zirconia. There are also two primary peaks observed in the reduction of Na/ZrO_2 . In agreement with the higher concentration of surface carbonate, the TPR peaks for reduction of Na/ZrO_2 are greater in area. They are also shifted to higher temperature relative to the ZrO_2 support, with positions at 525 and 725°C. The shift to higher temperature is attributed to interactions between Na and ZrO_2 which hinder the kinetics of the process. The addition of Pt to Na/ZrO_2 , not surprisingly, shifted the reduction peaks to lower temperature, though not as low as in the case of Pt/ZrO_2 (again, attributed to the Na- ZrO_2 interaction), with peaks situated at 225 and 450°C. The intensity of the peak at 450°C was verified by several tests. The higher intensity relative to the Na/ZrO_2 is likely attributed to the greater extent of reduction due to the presence of Pt. Both Na-doped catalysts exhibited higher intensity TPR peaks relative to their un-doped counterparts, which can be explained in part by the decomposition of carbonates, which were much higher in surface concentration.

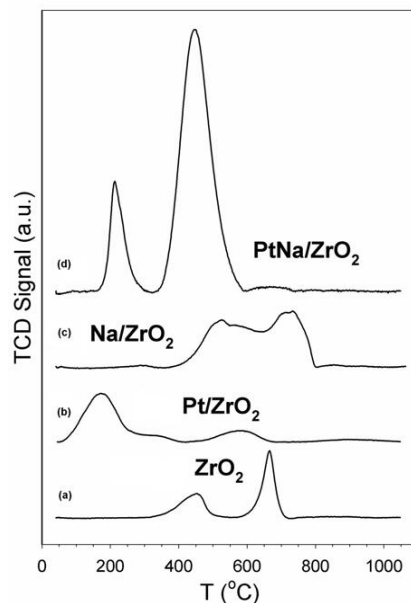


Figure 1: TPR profiles of, moving upward, high surface area zirconia (a), high surface area zirconia loaded with 2 % Pt (b), high surface area zirconia loaded with 2.5 % Na (c), and high surface area zirconia loaded with 2 % Pt and 2.5 % Na (d).

Results of CO adsorption at 300°C after catalyst activation for ZrO_2 , Pt/ZrO_2 , and PtNa/ZrO_2 are displayed in Figure 2. CO was observed to react with bridging OH groups (3715 - 3650 cm^{-1} range) to generate bands indicative of surface formate species. These bands included C-H stretching ($\nu(\text{C-H})$ 2880, minor bands 2966, 2745 cm^{-1}) and $\nu_{\text{as}}(\text{OCO})$ asymmetric (1568 cm^{-1}) and $\nu_{\text{s}}(\text{OCO})$ symmetric (1386, 1366 cm^{-1}) modes, for ZrO_2 and Pt/ZrO_2 catalysts. Pt/ZrO_2 was observed to exhibit higher intensity formate bands versus the ZrO_2 support. This is likely attributed to the role that Pt plays in facilitating the formation of reduced defect sites at low temperature^{8,9,13}. Additionally, CO adsorption also resulted in the formation of Pt-CO bands assigned to linear $\nu(\text{CO})$ (2069, 2050 cm^{-1}) and bridge-bonded $\nu(\text{CO})$ (1880 cm^{-1}) CO.

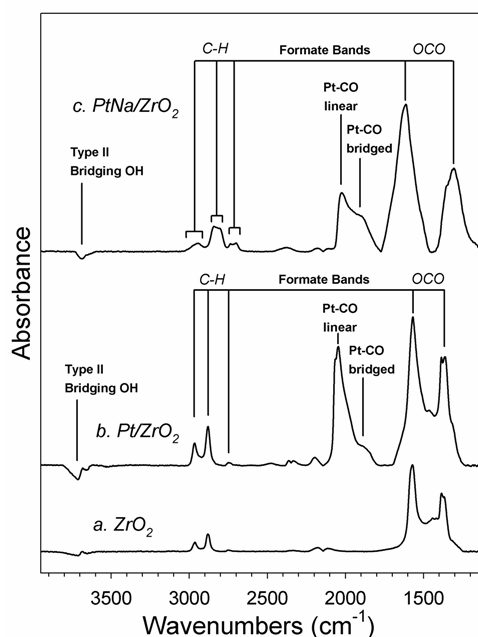


Figure 2: DRIFTS spectra of the adsorbed CO after activation in H_2 at $300^\circ C$ and purging in N_2 , moving upward, ZrO_2 (a), Pt/ZrO_2 (b), and $PtNa/ZrO_2$ (c). Conditions: $CO:N_2$ 3.75 $cm^3/min:130 cm^3/min$ at $300^\circ C$.

While the band positions for the formate species are virtually identical for the ZrO_2 and Pt/ZrO_2 catalysts, there are remarkable shifts in band positions when switching from Pt/ZrO_2 to $PtNa/ZrO_2$ catalyst. Firstly, there is an important change in the linear to bridge (i.e., L:B) Pt-CO ratio for the $\nu(CO)$ mode from 5:1 for Pt/ZrO_2 to 5:4, favoring bridge-bonded CO in the $PtNa/ZrO_2$ catalyst. Secondly, it is clear in this case that the alkali Na^+ influences not only the so-called Pt-CO L:B ratio²⁰, but also shifts the formate C-H bands to a lower wavenumber. This appears to be a result of the formate's interaction with Na.

At high H_2O/CO ratios, the rate of partially reducible oxides with precious metals (e.g., metal/ceria) has been suggested to be zero order in H_2O (i.e., whereby an adsorbed H_2O species is close to saturation), while that of CO is suggested to be first order, where the reaction rate essentially controls the coverage of the adsorbed CO intermediate⁵. In Figure 3 at $225^\circ C$, the coverage of the formate for the Pt/ZrO_2 and $PtNa/ZrO_2$ catalysts is very limited, while Pt-CO remains close to saturation during steady state. Note, that partial pressure of CO remains unchanged in Figure 3, and this suggests that the adsorbed CO intermediate is likely the formate species. Additionally during CO adsorption, the formate bands are higher in intensity for the $PtNa/ZrO_2$ catalysts, suggesting that the catalyst exhibits a higher population of active OH groups. The slightly higher intensity of the C-H bands for the Pt/ZrO_2 catalyst during water-gas shift, however, suggests that the formate is reacting more slowly relative to its Na promoted counterpart.

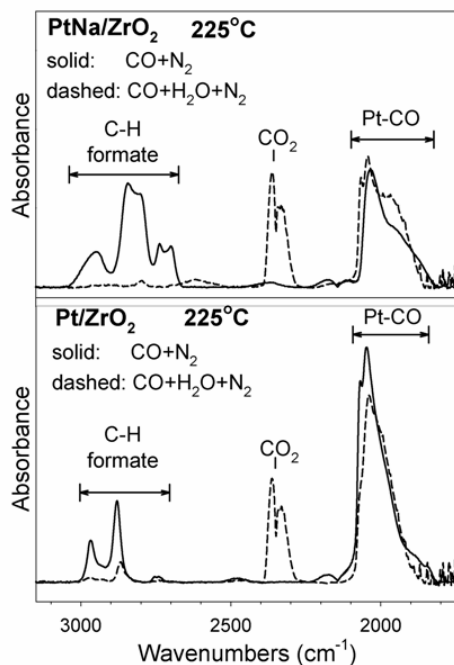


Figure 3: DRIFTS spectra of Pt/ZrO₂ (Bottom) and PtNa/ZrO₂ (Top) after CO adsorption (solid) at 225°C to H₂ activated catalysts and after switching to steady state water-gas shift conditions (dashed). Formate bands more reaction rate limited during WGS for Na-promoted catalysts, suggesting that formate is reacting faster. CO adsorption: 3.75 cm³/min CO:130 cm³/min N₂. Steady state WGS: 3.75 cm³/min CO:62.5 cm³/min H₂O:67.5 cm³/min N₂.

To explore the reactivity of the formate species further, the pseudo-stable formate was generated by CO adsorption to the H₂ activated catalyst, with cooling to 130°C. Transient decomposition of the formate was followed in steam as a function of time. Figure 4 provides a comparison of the transient formate decomposition fraction for Pt/ZrO₂ and PtNa/ZrO₂. Here, 20 % of the formate's initial intensity is decomposed in 5.2 min for Pt/ZrO₂ and 2.4 min for PtNa/ZrO₂, suggesting that the formate is more reactive for the Na-promoted catalyst.

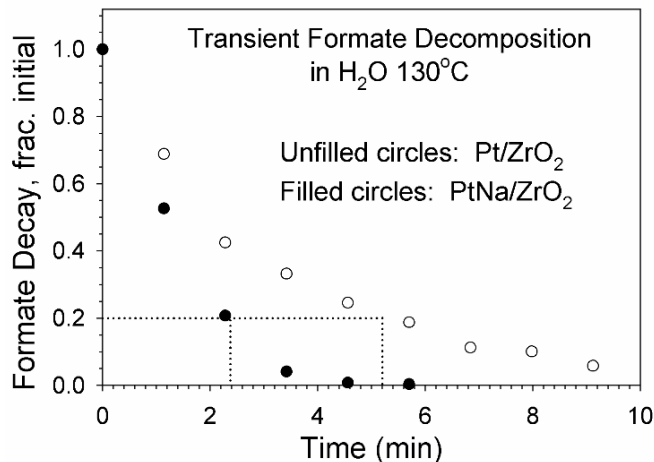


Figure 4: Formate area response to steaming at 130°C in H₂O:N₂ 62.5 cm³/min:67.5 cm³/min for Pt/ZrO₂ (Unfilled circles) and PtNa/ZrO₂ (Filled circles). The 0.20-life of formate is indicated for each case, demonstrating a faster rate for PtNa/ZrO₂. Forward decomposition.

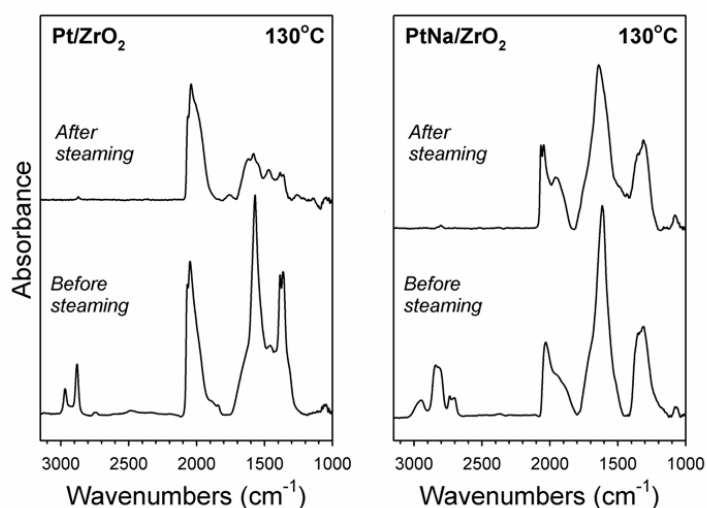


Figure 5: Before and after transient formate decomposition in H₂O at 130°C, including Pt/ZrO₂ (Left) and PtNa/ZrO₂ (Right).

Interestingly, the carbonates ($\sim 1850 - 1300 \text{ cm}^{-1}$) are very low for the Pt/ZrO₂ after steaming (Figure 5, left), consistent with the observed CO₂ evolution for that sample (see Figure 3). In contrast, the carbonates are retained on the surface of PtNa/ZrO₂ at 130°C (Figure 5, right), and it is interesting to note that more carbonate was retained on the surface of the PtNa/ZrO₂ catalyst after H₂ activation, too (see Figure 6, top). A close-up of the carbonates generated from the formate decomposition of Pt/ZrO₂ is also provided (Figure 6, bottom).

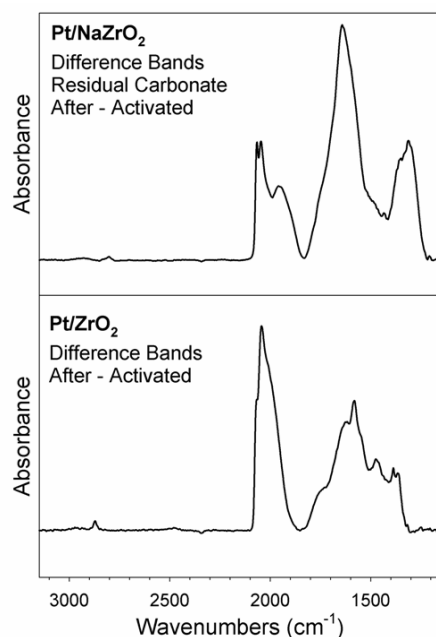


Figure 6: The resultant difference bands for after - activated for Pt/ZrO₂ and PtNa/ZrO₂ (right). Note that for Pt/ZrO₂, little formate and carbonate remains, consistent with CO₂ evolution (see Figure 3). However, for PtNa/ZrO₂, significant carbonate residual remains on the surface after formate decomposition at 130°C.

Conclusions

As explored by infrared spectroscopy, CO adsorption at 300°C displayed the C-H stretching bands indicative of the formate species for ZrO₂, Pt/ZrO₂ and PtNa/ZrO₂. Additionally, Pt/ZrO₂ and PtNa/ZrO₂ demonstrated higher intensity of formate than compared to ZrO₂ alone. More notable change was the red-shifting C-H bands of the Na doped sample suggesting a weakening of the C-H bond, which has been proposed to be the rate-limiting step of the low temperature water-gas shift mechanism. First, steady state water-gas shift testing at 225°C indicated that the coverage of formate was more limited for the PtNa/ZrO₂ catalyst compared to Pt/ZrO₂, suggesting that it was reacting faster. Secondly, in transient formate decomposition tests at 130°C in steam, forward decomposition to carbonate species was observed, and the formates on PtNa/ZrO₂ decomposed to 20 % of their initial value in 1/2 the time in comparison with Pt/ZrO₂.

References

- (1) C.J. Brooks, A. Hagemeyer, K. Yaccato, R. Carhart, M. Herrman, A. Lesik, P. Strasser, A. Volpe, H. Turner, and H. Weinberg, 19th Meeting of the North American Catalysis Society, Philadelphia, Pennsylvania, May 22-27, 2005.
- (2) T. Shido and Y. Iwasawa, *J. Catal.* 141 (1993) 71.
- (3) S. Hilaire, X. Wang, T. Luo, R.J. Gorte, J. Wagner, *Appl. Catal.* 215 (2001) 271.
- (4) T. Bunluesin, R.J. Gorte, G.W. Graham, *Appl. Catal. B: Environ* 15 (1998) 107.
- (5) Y. Li, Q. Fu, M. Flytzani-Stephanopoulos, *Appl. Catal. B: Environ.* 27 (2000) 179.

- (6) G. Jacobs, L. Williams, U.M. Graham, D.E. Sparks, B.H. Davis, *Appl. Catal. A* 252 (2003) 107.
- (7) G. Jacobs, U.M. Graham, E. Chenu, P.M. Patterson, A. Dozier, B.H. Davis *J. Catal.* 229 (2005) 499.
- (8) S.M. Stagg-Williams, D.E. Resasco, *Stud. Surf. Sci. Catal.* 130 (2000) 3663.
- (9) F.B. Noronha, C. Taylor, E.C. Fendley, S.M. Stagg-Williams, D.E. Resasco, *Catal. Lett.* 90 (2003)
- (10) C. Binet, M. Daturi, J.C. Lavalley, *Catal. Today* 50 (1999) 207.
- (11) G. Jacobs, P.M. Patterson, L. Williams, D. Sparks, and B.H. Davis, *Catal. Lett.* 96 (2004) 97.
- (12) C. Li, K. Domen, K. Maruya, T. Onishi, *J. Catal.* 125 (1990) 445.
- (13) J. El Fallah, S. Boujana, H. Dexpert, A. Kiennemann, J. Marjerus, O. Touret, F. Villain, F. Le Normand, *J. Phys. Chem.* 98 (1994) 5522.
- (14) G. Jacobs, A.C. Crawford, and B.H. Davis, *Catal. Lett.* 100 (2005) 147.
- (15) J. Lamotte, J.C. Lavalley, E. Druet, E. Freund, *J. Chem. Soc., Faraday Trans.* 79 (1983) 2219.
- (16) K. Jung, A.T. Bell, *J. Catal.* 193 (2000) 207.
- (17) J. Kondo, Y. Sakata, K. Domen, K. Maruya, T. Onishi, *J. Chem. Soc., Faraday Trans.* 86 (1990) 397.
- (18) G. Jacobs, P.M. Patterson, U.M. Graham, A.C. Crawford, A. Dozier, and B.H. Davis, *J. Catal.* 235 (2005) 79.
- (19) E. Chenu, G. Jacobs, A.C. Crawford, R.A. Keogh, P.M. Patterson, D.E. Sparks, and B.H. Davis, *Appl. Catal. B: Environ.* 59 (2005) 45.
- (20) B.L. Mojet, J.T. Miller, and D.C. Koningsberger, *J. Phys. Chem. B* 103 (1999) 2724.